NUCL SCI TECH (2019) 30:123
https://doi.org/10.1007/s41365-019-0648-5

Conceptual design and update of the 128-channel μSR prototype spectrometer based on musrSim

Zi-Wen Pan[1] · Jing-Yu Dong[1] · Xiao-Jie Ni[1] · Lu-Ping Zhou[2,3] · Jing-Yu Tang[2] · Daniel E. Pooley[4] · Stephen P. Cottrell[4] · Bang-Jiao Ye[1]

Received: 10 December 2018 / Revised: 16 April 2019 / Accepted: 17 April 2019 / Published online: 12 July 2019

Abstract An experimental muon source (EMuS) will be built at the China Spallation Neutron Source (CSNS). In phase I of CSNS, it has been decided that EMuS will provide a proton beam of 5 kW and 1.6 GeV to generate muon beams. A 128-channel muon spin rotation/relaxation/resonance (μSR) spectrometer is proposed as a prototype surface muon spectrometer in a sub-branch of EMuS. The prototype spectrometer includes a detection system, sample environment, and supporting mechanics. The current design has two rings located at the forward and backward directions of the muon spin with 64 detectors per ring. The simulation shows that the highest asymmetry of approximately 0.28 is achieved by utilizing two 10-mm-thick brass degraders. To obtain the optimal asymmetry, the two-ring structure is updated to a four-ring structure with 32 segments in each ring. An asymmetry of 0.42 is obtained through the simulation, which is higher than that of all the current μSR spectrometers in the world.

Keywords EMuS · μSR spectrometer · 128-Channel · Two-ring structure · Four-ring structure · Asymmetry

1 Introduction

The μSR technique uses a highly spin-polarized muon beam ($\sim$ 100% for surface muons) to probe the structure and dynamics of condensed matter. In this technique, polarized muons are implanted into a sample where their polarization evolves in the local magnetic field, and they decay with a lifetime of 2.2 μs. By collecting millions of decay positrons, one can reconstruct the time independence of the muon spin depolarization function, which reflects the spatial and temporal inhomogeneities of the local magnetic field at the muon site [1]. Owing to the sensitivity of muons to magnetic fields, the μSR technique has been widely used in studying magnetic systems, superconductors, particle transport in matter, semiconductors, etc. [2, 3].

Currently, only four muon facilities in the world (PSI/SμS [4, 5], TRIUMF/CMMS [6], ISIS Muon Source [7], and J-PARC/MUSE [8]) can conduct μSR experiments. The muon sources at ISIS and J-PARC are in pulsed mode. The entire muon intensity can be used for a pulsed beam. Therefore, there is almost no background in the μSR signal. This capability renders the pulsed muon beam suitable for studying wake magnetic fields. The muon facilities in PSI and TRIUMF use continuous muon beams (continuous wave, CW). The time resolution of the μSR signal in the CW mode can be considerably small ($\sim$ 100 ps) with an appropriate choice of detection and electronic systems.

This work was supported by the National Natural Science Foundation of China (No. 11527811) and the Key Program of State Key Laboratory of Particle Detection and Electronics. A part of the work performed in the UKRI ISIS Detector Group was sponsored by the China Scholarship Council.

✉ Bang-Jiao Ye
bjye@ustc.edu.cn

1 State Key Laboratory of Particle Detection and Electronics, University of Science and Technology of China, Hefei 230026, China

2 Institute of High Energy Physics, Chinese Academy of Sciences, Beijing 100049, China

3 University of Chinese Academy of Sciences, Beijing 100049, China

4 ISIS Facility, STFC Rutherford Appleton Laboratory, Chilton, Oxfordshire OX11 0QX, UK

Therefore, strong magnetic fields and fast relaxing effects can be detected in these muon facilities. The muon beams at these institutions are complementary [1, 2]. A new muon facility, MuSIC [9], is being developed for μSR applications. Owing to the increasing demands of μSR applications, new muon beams, i.e., experimental muon source (EMuS) [10–12], at China Spallation Neutron Source (CSNS) and RAON [13] in South Korea are under construction. EMuS was proposed to be an extended platform for muon science, which will be a standalone facility and will use approximately 5% (5 kW, 2.5 Hz) of the total proton beam power. Since 2007, preliminary R&D efforts have been undertaken. EMuS will provide pulsed muons to μSR experiments. With the recent completion of the CSNS project in March 2018, the construction of the EMuS facility has become more realistic [14].

A spectrometer is a key instrument in μSR experiments. For pulsed muon beams, the μSR spectrometer should cover a sufficient solid angle to obtain a high count rate to reduce the detection time. A high asymmetry should be achieved to quantify the performances of a spectrometer. Most muons decay in early time in each bunch. Hence, the detection system will face a pileup problem in early time. Accordingly, the detection system is usually split into many segments. The μSR spectrometers in ISIS have 96/64/64 segments, which can accept an event rate of 40–200 million events per hour (MEvents/h) depending on slit settings and degraders [7]. The μSR spectrometers in J-PARC have 256/1280 segments, accepting 40/180 MEvents/h [15]. The maximum asymmetries of the three spectrometers in ISIS are up to 0.28 through the use of degraders [7]. The asymmetries of the spectrometers in J-PARC are approximately 0.16, which is low owing to the high angle (51°–60°) of the detectors with respect to the muon spin direction [15]. The repetition rate of EMuS is 2.5 Hz, and the muon beam intensity is optimized to 1.44×10^5 muons/s. Owing to the limited number of detector segments (128 channels) and low repetition rate, the event rate of the μSR spectrometer will be lower than those of ISIS and J-PARC. For a general-purpose μSR spectrometer, the asymmetry is typically 0.2–0.25. The asymmetry is the main parameter from which the magnetic information of materials can be derived [1]. If the asymmetry can be improved to 0.4, good statistical accuracy can be achieved with a low event rate: The figure of merit of a μSR experiment is given by A^2N, where A is the asymmetry and N is the total number of detected events. To accept a relatively high muon beam intensity and achieve good statistical accuracy, the prototype spectrometer is updated from a two-ring structure with an asymmetry of ~ 0.28 to a four-ring structure to achieve the optimal asymmetry of up to 0.42.

2 Models and methods

The μSR spectrometer is simulated using two toolkits. First, the responses of the detection system to decay positrons are simulated using musrSim [16] based on Geant4 [17] and ROOT [18]. Users can build geometries, external magnetic fields, and particle vertexes in a macro file and allow it to be run by musrSim. Here, musrSim simplifies the coding of Geant4. The simulation result of musrSim is output into a ROOT file. Once the simulation is completed, users can use another toolkit, i.e., musrSimAna [16], to analyze the output ROOT files.

2.1 Model description

Figure 1 shows the schematics of the μSR prototype spectrometer built in musrSim. In the upper part of Fig. 1, the two-ring structure comprises two detector rings with 64 detectors per ring, degraders, a cryostat, and a beam pipe. The new four-ring structure (bottom) changed the cryostat to a close cycle refrigeration (CCR) system with cruciform similar to that of the European Muon (EMU) spectrometer [19]. The four-ring spectrometer has 32 detectors per ring, resulting in a reduction in the radius of the detector ring from 150 to 90 mm. The arrangement of detectors in this four-ring structure is similar to that of the EMU spectrometer. Table 1 presents the main parameters of these two models. The optimal size of the degraders is described in Sect. 3. Note that the detector ring near the sample is assigned as the inner ring. Five million muons were simulated in each run to obtain good statistical precision. The sample size used in the ISIS muon facility generally ranges from 10 to 50 mm (in both horizontal and vertical directions). Therefore, we set the size of the sample to Φ30 mm. The parameters of the EMuS beam are listed in Table 1. The size of the muon beam spot on the sample is optimized to 30×30 mm^2 in full width at half maximum (FWHM) accordingly. A small beam spot can be achieved by modifying slit settings if required in a specific experiment.

Figure 2 shows the RMS envelope of the EMuS muon beam. Solid lines are provided by the accelerator group of EMuS at CSNS, which is simulated using g4bl (G4Beamline) [20]. The spatial and angular distributions of the beam are set up in musrSim consistent with g4bl simulations (dots in Fig. 2).

2.2 Asymmetry of a μSR spectrometer

For a bunch of surface muons, their decay positrons emit asymmetrically but preferentially along the polarization. The angular distribution [21] of positrons is

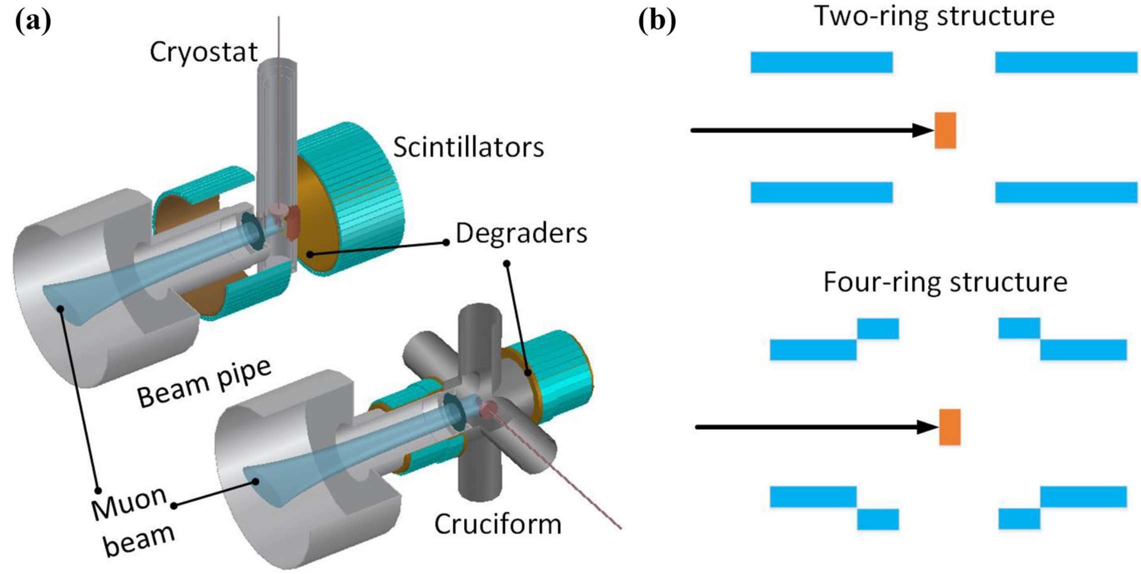

Fig. 1 (Color online) Illustrations (cutting view) of a 128-channel μSR prototype spectrometer. **a** Upper: two-ring structure (*Φ*300-mm detector ring), bottom: four-ring structure (*Φ*180-mm detector ring); **b** projection of detector rings along the *z*-axis

Table 1 Main parameters of the simulation model in musrSim

	Two-ring structure	Four-ring structure
Number of rings	2	4
Segments per ring	64	32
Radius of one ring (mm)	150	Inner: 95, outer: 90
Scintillator material	Plastic (EJ200)	Plastic (EJ200)
Scintillator size (mm^3)	13.5 × 5 × 175	Inner: 18 × 5 × 40
		Outer: 17 × 5 × 100
Sample environment	Cryostat + sample plate	CCR + fly-past
Beam parameters		
Intensity (muons/s)	1.44×10^5	
Beam spot (mm × mm, FWHM)	30 × 30	
Beam emittance (π·mm·mrad)	491 × 210	

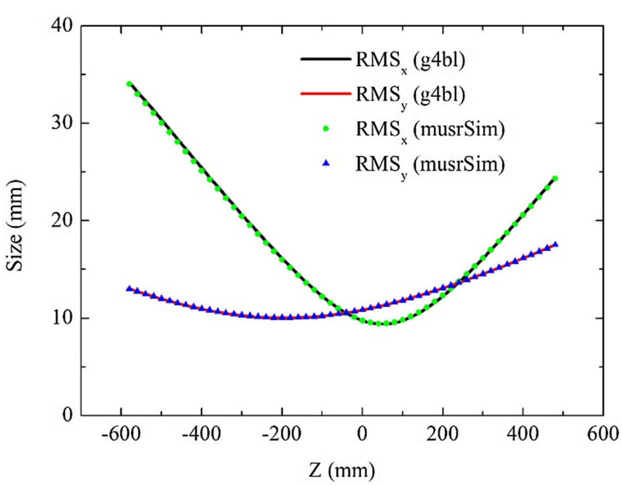

Fig. 2 (Color online) RMS envelope of the EMuS muon beam with a spot size of 30 × 30 mm^2

$$dW/d\cos\theta = 1 + A(x)\cos\theta,$$
$$A(x) = (2x - 1)/(3 - 2x), \tag{1}$$

where A denotes the asymmetry and x is the ratio of the positron's kinetic energy to the maximum energy 52.8 MeV. The asymmetry $A(x)$ is the asymmetry for a well-defined positron energy x. In an experiment, the observable asymmetry of a spectrometer is larger than 0 integrating over all the measured positron energies. A higher statistical precision can be achieved if a spectrometer has a high asymmetry. According to Eq. (1), high-energy positrons ($x > 0.5$) have a positive decay asymmetry, and their emission angles with respect to the muon spin become smaller. Degraders can be used to block low-energy positrons ($x < 0.5$) to increase the observable asymmetry of the spectrometer.

For a ZF/TF (zero field/transverse field) case, the asymmetry is determined by

$$\alpha = \left(N_{\mathrm{B}}^{+} + N_{\mathrm{B}}^{-}\right)/\left(N_{\mathrm{F}}^{+} + N_{\mathrm{F}}^{-}\right), \tag{2}$$

$$A^{\pm} = \left(N_{\mathrm{B}}^{\pm} - \alpha N_{\mathrm{F}}^{\pm}\right)/\left(N_{\mathrm{B}}^{\pm} + \alpha N_{\mathrm{F}}^{\pm}\right), \tag{3}$$

where the "plus sign" indicates the muon polarization parallel to the forward detector ring and the "negative sign" indicates the antiparallel case; B and F denote the detector rings in the downstream or upstream direction along the beam direction, respectively. For a TF simulation, muons are precessing in a transverse field applied in the vertical direction in the sample area, and the asymmetry can be derived by directly fitting μSR "spectra" with

$$f(t) = N_0 \exp\left(-t/\tau_{\mu}\right)[1 + A\cos(\omega t + \varphi_0)] + B, \tag{4}$$

where N_0 is the initial muon count, τ_{μ} is the lifetime of the muon, ω is the angular frequency dependent on the gyromagnetic ratio of the muon and the strength of the field, ϕ_0 is the initial phase, and B is the background.

2.3 Energy threshold of a detector

As the scintillator is thin (5 mm), over 99% positrons penetrate the detector. The energy loss spectrum is given by the Landau distribution as shown in Fig. 3. The energy threshold can be set to 0.8 MeV to discriminate events with lower energy deposition. These events are due to low-energy positron events, gamma events, or PM tube noise.

3 Results and discussion

3.1 Validation of the simulation model

A detector module of the two-ring structure was tested on the EMU spectrometer at the ISIS Muon Source. During the test, an EMU detector module (consisting of three segments) was replaced by the Chinese detector as shown in Fig. 4a. Figure 4b shows the result obtained from the experiment. The asymmetry is fitted by 0.2540 ± 0.0017. The single Chinese detector was also modeled in musrSim. Here, 10^7 muons were simulated for this specific experiment. The polarization of the ISIS muons is over 99%. Therefore, the polarization of the muons in the simulation is set to 100%. The simulated asymmetry is fitted by 0.2547 ± 0.0073 (Eq. (4)), which is consistent with the experiment. Details of optimization of this two-ring spectrometer are described in [22].

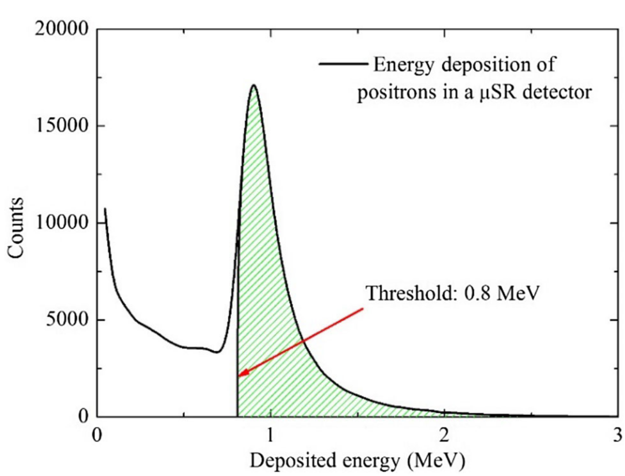

Fig. 3 (Color online) Energy deposition spectrum in a detector module

3.2 Influence of degrader materials on the asymmetry

Four types of metals were chosen as degrader materials as shown in Fig. 5. The asymmetry has a peak value when the degrader thickness changes. According to Eq. (1), the asymmetry has the range [− 0.33, 1] and positrons with kinetic energy = 26.4 MeV have zero asymmetries. When the thickness of the degrader is small, low-energy positrons can be blocked, resulting in an increase in asymmetry. Thereafter, the asymmetry drops. This is because multiple scattering changes the angular distribution of positrons if the degrader becomes thicker. The similarity of peak values in Fig. 5 indicates that the gain effects of different materials are almost the same. Lead is soft and toxic. Tungsten is more expensive than brass. Aluminum requires more material to obtain the same asymmetry as that of brass. From the simulation, brass has slightly higher asymmetry. Therefore, brass was set as the degrader material in subsequent simulations.

3.3 Optimizing the two-ring structure

As mentioned in Sect. 2.1, a cryostat is used in the two-ring structure as the sample environment. The sample is fixed on a large sample plate (made of silver). As the beam spot is large, samples with sizes of Φ30 mm and Φ40 mm are simulated. As shown in Fig. 6a, approximately 80% and 60% detected positrons are decayed from the Φ40-mm and Φ30-mm samples, respectively. Reduced positron events from the sample are transferred into the sample plate. Positrons decayed from outside the sample will be detected by the spectrometer as background. To eliminate the influences of these backgrounds, the cryostat can be updated to a fly-past structure, and a small silver sample plate can be used. The fly-past structure can allow muons outside the sample through the spectrometer. It is beneficial to small samples [19] depending on the beam divergence. Silver has no electronic moment and has very small nuclear moments. Background positrons from the silver plate can be separated from any relaxing signals from a sample as the

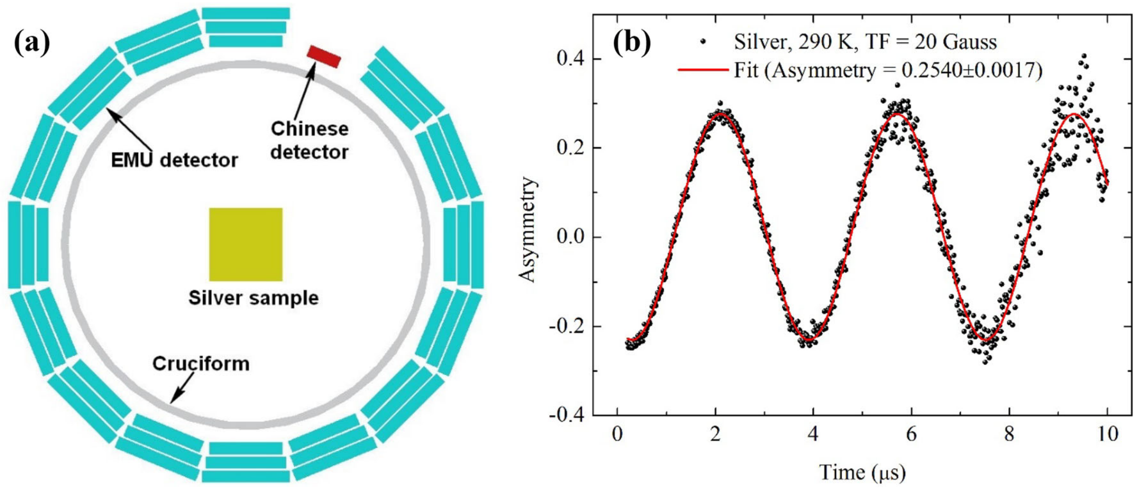

Fig. 4 (Color online) **a** Location of the Chinese detector, **b** asymmetry of the TF test

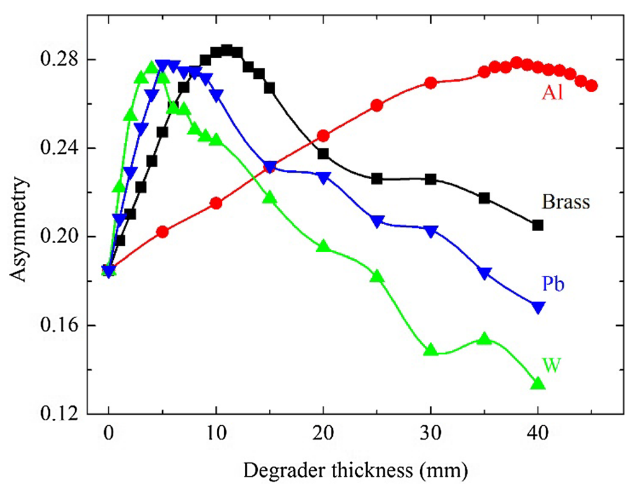

Fig. 5 (Color online) Variation of simulated asymmetry with degrader thickness

background is non-relaxing. However, for very low sample depolarization rate comparable to that of silver, the two components cannot be separated. Hence, measurements at very low sample depolarization rate are limited. Increasing the percentage of muons decaying inside the sample is important for reducing the background. Percentages of decayed positrons have no significant differences in the ZF (a) and TF (b) conditions.

The calculation of asymmetry with or without a cryostat in ZF/TF is shown in Fig. 6c, d. The cryostat is a three-layered structure (each layer is a 1.5-mm-thick aluminum layer) [23]. Windows on the cryostat with an aperture of 55 mm are made of Mylar film (total thickness of 25 mm). For a certain sample size, the asymmetry with a cryostat is higher than that without one. This is because the cryostat can be considered a degrader, which can block low-energy positrons with low asymmetries. This is because, as the position of the sample does not change, asymmetries related to different sizes are approximately the same. However, if the beam emittance is large, muons passing the sample may hit a degrader, resulting in a reduction in the asymmetry. The asymmetry in the TF condition (d) is smaller than that in the ZF condition (c). The reason is that the spin rotates in the TF condition, making the average emission symmetrical axis tilt to the z-axis. According to the simulation, the highest asymmetry obtained by this two-ring structure is 0.28 with 10-mm-thick brass degraders.

For a μSR spectrometer with FPGA readout electronics, each detector detects approximately 10 events/pulse, which is tolerable to the distortion of positron time spectra [19]. Hence, the acceptance of the beam for the 128-channel spectrometer is 128 × 10 × repetition rate/detection efficiency/beam intensity. Table 2 lists the detection efficiency and acceptance for two sample sizes. Less than one-fifth of the beam can be accepted by the spectrometer. If the two-ring spectrometer is operated under this beam, a pileup of signals will lead to significant distortions of μSR spectra, which cannot be corrected. The two-ring spectrometer must be updated to a four-ring one to obtain a higher asymmetry and accept the full beam intensity.

3.4 Scanning the asymmetry along the z-axis

Figure 7 shows the projection of the detector rings in the Y–Z plane. According to Eq. (1), the asymmetry of these two rings can be calculated by

$$\text{Asymmetry} = \bar{A}(\cos\theta_1 + \cos\theta_2)/2, \quad (5)$$

where $\bar{A}$ is the asymmetry for an infinitesimally small solid angle ($\Theta_1 \approx \Theta_2 \approx 0$) averaged over all the positron

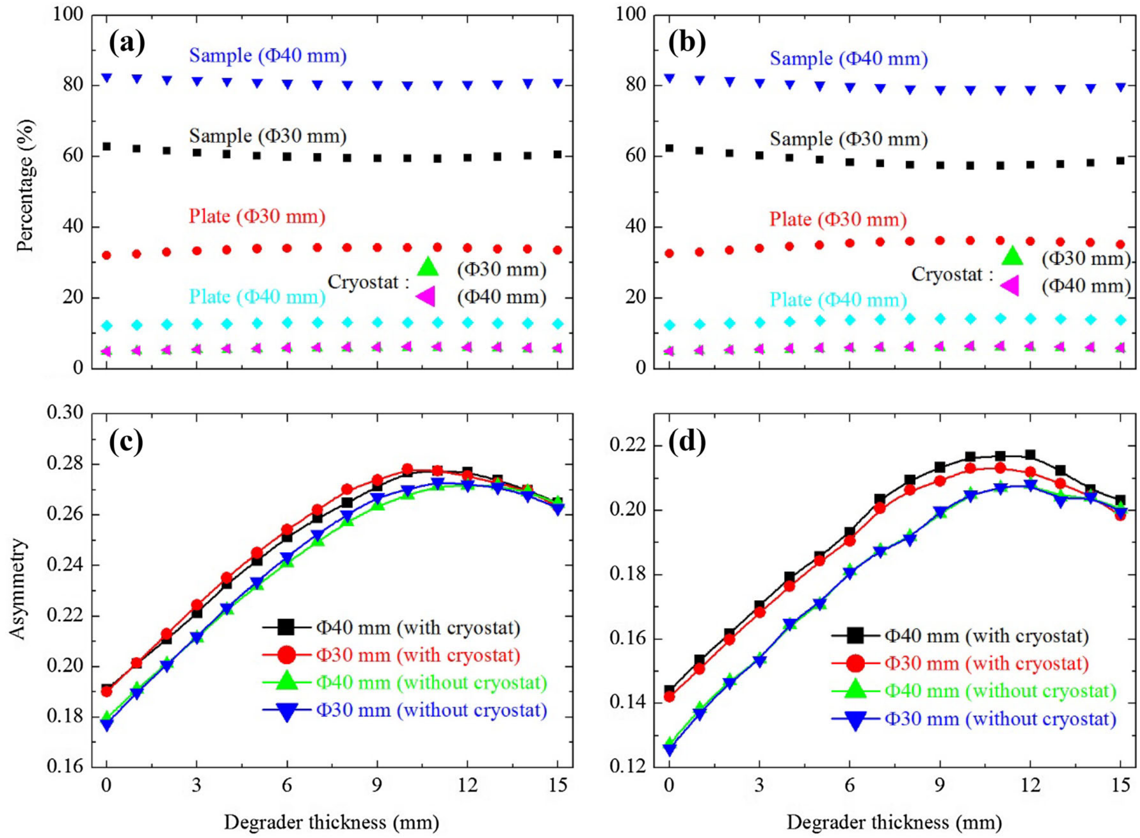

Fig. 6 (Color online) Variation of percentages of detected positrons decayed from different parts (**a**, **b**) and asymmetries (**c**, **d**) with the brass degrader thickness. **a**, **c** are for ZF and **b**, **d** are for TF (100 Gauss)

Table 2 Detection efficiency and acceptance of the beam with different sample sizes

Sample size (mm)	Detection efficiency (%)	Acceptance of the beam (%)
*Φ*40	11.53	19.27
*Φ*30	12.16	18.27

energies accepted by the spectrometer. Without degraders, i.e., accepting positron energies from close to zero up to the maximum energy, the average asymmetry $\bar{A} = 0.33$. With a degrader, the minimum accepted positron energy will be considerably larger than 0, resulting in $\bar{A} > 0.33$. The formula indicates that, if the radius is small or the detector ring is far away from the sample, indicating that Θ_1 or Θ_2 is small, high asymmetry can be achieved. It also indicates that the asymmetry cannot be higher than $\bar{A}$.

Simulations of scanning the asymmetry along the *z*-axis were performed with the detector length of 10 mm (radius of the detector ring = 150 mm or 90 mm) to verify the relation between the asymmetry and location. For these specific simulations, 10^7 muons were simulated to suppress statistical fluctuations. Ideally, a virtual detector with zero length can exactly detect the asymmetry in each point along the *z*-axis according to Eq. (5). However, we cannot determine the energy deposition used to confirm whether

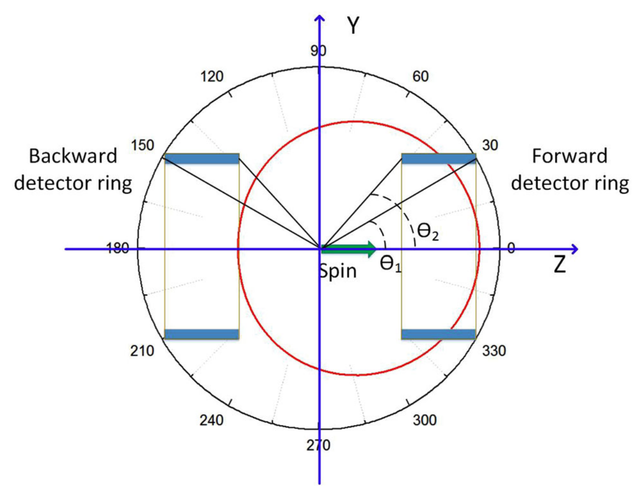

Fig. 7 (Color online) Projection of detector rings along the spin. The red circle is the angular distribution of positrons averaged over all the positron energies

the deposited event is a muon decay event. A detector with a length of 10 mm is sufficiently small to detect the asymmetry in its location. For the two-ring structure, each ring has 64 scintillators (see Table 1). The width of each segment is 13.5 mm, resulting in the detector ring with a radius of 150 mm. For the four-ring structure, each ring has 32 detectors. Similar to the fly-past device in EMU, the radius of the cruciform (see Fig. 1) is approximately 80 mm. Detectors should be placed outside the cruciform or degraders. Therefore, the minimum radius of the detector ring that can be chosen is 90 mm. Figure 8 shows scanning of the asymmetry using degraders with different thicknesses along the z-axis in the ZF. Theoretical results were calculated using Eq. (5). The simulation results in Fig. 8 are consistent with their corresponding theoretical ones. The space occupied by the spectrometer is in the region (− 350, 350) mm along the z-axis. In this region, detectors that use thicker degraders can achieve higher asymmetries. When detectors are further away from the sample, higher asymmetries can be achieved but the asymmetry increases slowly after z = 150 mm. Comparing detector rings with different radii but the same degrader thickness, asymmetries increase quickly with a smaller radius (90 mm). Furthermore, detectors with smaller radius can achieve higher asymmetries in the interested region along the z-axis. To achieve high asymmetries, the two-ring spectrometer should be updated to a four-ring one. According to the analysis, a detector ring can be placed after 150 mm to achieve the highest asymmetry and another detector ring can be mounted before 150 mm to cover more solid angle for the four-ring spectrometer. Therefore, the outer detector ring with a length of 100 mm is set up after 150 mm. To ensure that the inner and outer rings have the same covered solid angle, the length of the inner ring is set to 40 mm.

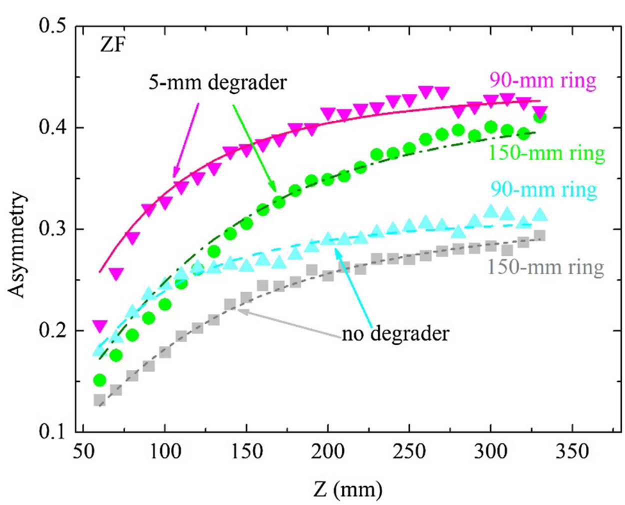

Fig. 8 (Color online) Asymmetries of 10-mm-long detector rings (radius = 90 mm or 150 mm) using brass with different thicknesses in varied locations. Curves are calculated using Eq. (5)

3.5 Optimizing the four-ring structure

As discussed in Sect. 3.3, the sample environment should use a fly-past structure. Hence, the diameter of the sample plate is the same as that of the sample. Muons outside the sample can pass through the cruciform without any obstructions. Samples with four sizes were simulated to determine the influences of the sample size and the beam emittance on the asymmetry. Figure 9 shows the percentages of positrons decayed from the sample with different sizes. If the diameter of a sample is not smaller than Φ20 mm, over 93% positrons are decayed from the sample. Accordingly, the largest sample (Φ30 mm) has the highest asymmetry (approximately 0.42) and the asymmetry does not change significantly for a reduction in the sample size from Φ30 mm to Φ20 mm as shown in Fig. 10a. If a sample is small (Φ15 mm or Φ10 mm), the percentage of positrons from the sample and the observable asymmetry reduces significantly. This is because the angular dispersion of the real beam is relatively large for small samples. Muons passing through the sample could hit the inner wall of the cruciform or degrader in the right side of the sample as shown in the bottom part of Fig. 1. However, asymmetries for samples of different sizes are almost the same in the TF condition (Fig. 10b). Asymmetry of the inner or outer ring is also plotted in Fig. 10c, d. The outer ring has higher asymmetry than the inner ring (up to $\sim$ 13% in ZF and $\sim$ 18% in TF). This is because high-energy positrons emit preferentially along the z-axis, indicating that the emission angle of these high-asymmetry positrons is small. The angle of the outer ring pointing to the sample is smaller than that of the inner ring. Therefore, the outer

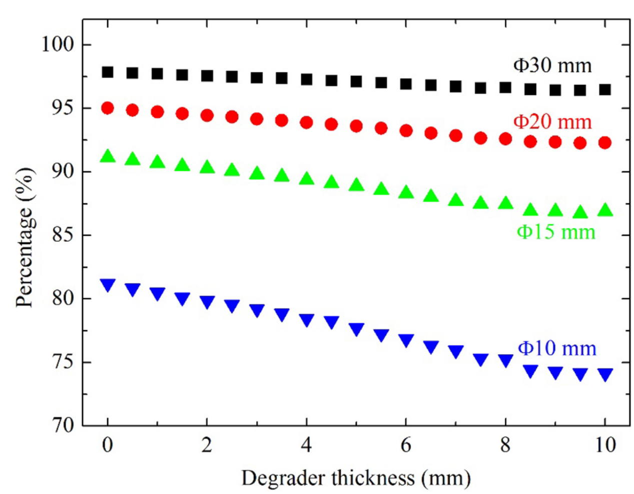

Fig. 9 Percentage of positrons decayed from samples with four sizes in ZF

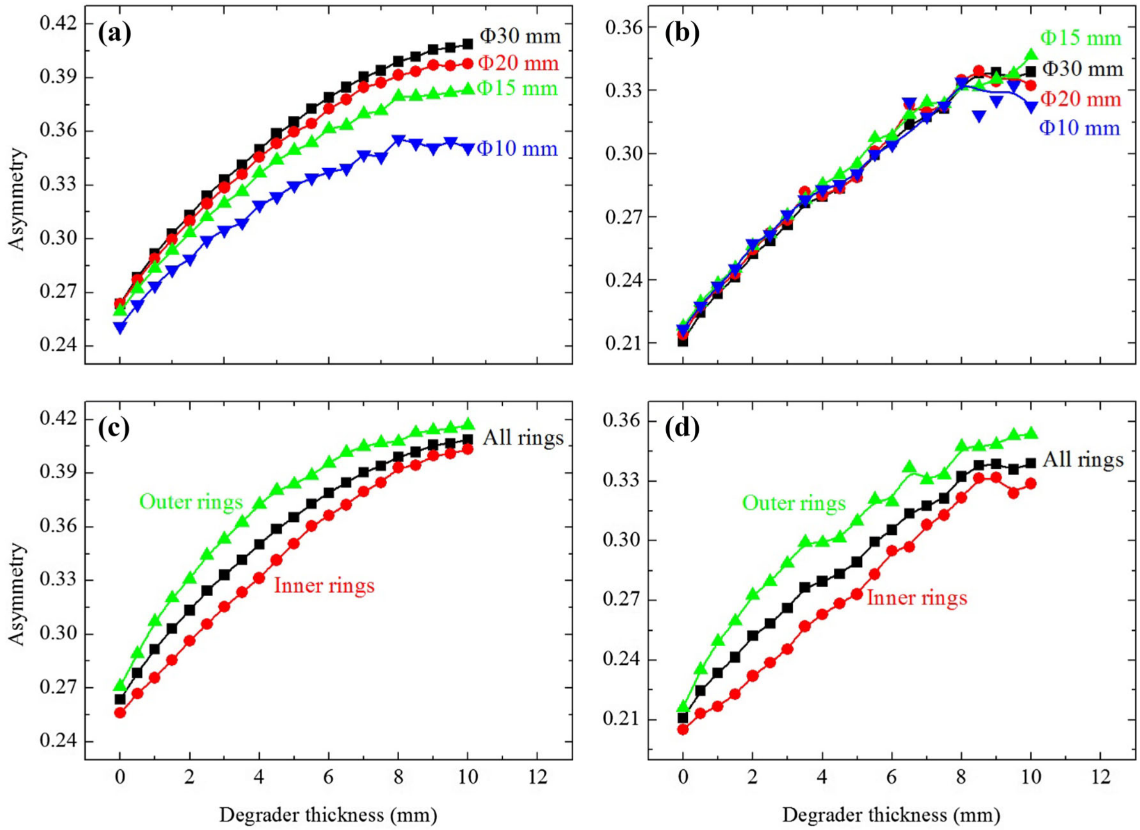

Fig. 10 (Color online) Observable asymmetry as a function of the degrader thickness in ZF (**a**, **c**) and TF (**b**, **d**). Curves are eye-guide lines

Table 3 Detection efficiency and average count rate of each ring for Φ30-mm sample

	Detection efficiency (%)	Mean count rate (counts/pulse/detector)
All rings	2.10	9.43
Inner ring	1.22	10.96
Outer ring	0.88	7.90

detectors can achieve higher asymmetries. From these simulations, the optimal degrader thickness is 10 mm.

Table 3 shows the detection efficiency and mean count rate per pulse per detector. From Fig. 10 and Table 3, it can be observed that the four-ring structure can achieve the highest asymmetry ($\sim$ 0.42) and also accept a relatively high muon beam intensity.

4 Conclusion

The simulation model was validated with the beam test for the one-channel prototype spectrometer. The simulation is consistent with the experiment. The covered solid angle of a detector determines the asymmetry. A detector ring with a fixed length can achieve high asymmetry if it is placed far away from the sample. (The angle of the detector pointing to the sample is small.) A detector ring with smaller radius can achieve higher asymmetry in the same location along the z-axis. For the current beam parameters (spot and emittance), a fly-past structure for samples with sizes not smaller than 15 mm can reduce the background significantly. A two-ring and 128-channel μSR prototype spectrometer was optimized to achieve the highest asymmetry of 0.28. However, it cannot accept a high-intensity muon beam and faces large background when using a large sample plate and cryostat. Therefore, the two-ring structure was updated to a four-ring structure to achieve higher asymmetry. Furthermore, the cryostat was updated to a fly-past device to reduce the background signals. The four-ring prototype spectrometer was optimized, with the highest asymmetry of approximately 0.42. Each detector can detect approximately ten events per pulse so that early-time distortions in the muon decay histograms can be neglected or corrected. The four-ring μSR spectrometer can accept the currently designed muon intensity of 1.44×10^5 muons/s.

5 Acknowledgements

We thank the China Newton Fund for financial support and ISIS, STFC, UK, for the beamtime to conduct these muon experiments [24]. The authors would like to thank Adrian Hillier, Nigel Rhodes, James Lord, Peter Baker, and colleagues of the EMuS group for their useful comments and valuable suggestions.

References

1. P. Dalmas de Réotier, A. Yaouanc, Muon spin rotation and relaxation in magnetic materials. J. Phys.: Condens. Matter **9**, 9113–9166 (1997). https://doi.org/10.1088/0953-8984/9/43/002
2. J.E. Sonier, μSR brochure (2002). http://musr.net/muSR Brochure.pdf
3. P.J.C. King, R. Renzi, S.P. Cottrell et al., ISIS muons for materials and molecular science studies. Phys. Scr. **88**, 068502 (2013). https://doi.org/10.1088/0031-8949/88/06/068502
4. F. Foroughi, E. Morenzoni, T. Prokscha et al., Upgrading the PSI muon facility. Hyperfine Interact. **138**, 483–488 (2001). https://doi.org/10.1023/A:1020830830050
5. R. Xiao, E. Morenzoni, Z. Salman et al., A segmented conical electric lens for optimization of the beam spot of the low-energy muon facility at PSI: a Geant4 simulation analysis. Nucl. Sci. Tech. **28**, 29 (2017). https://doi.org/10.1007/s41365-017-0190-2
6. J.L. Beveridge, J. Doornbos, D.M. Garner, Muon facilities at TRIUMF. Hyperfine Interact. **32**, 907–912 (1986). https://doi.org/10.1007/BF02395002
7. A.D. Hillier, M. Aramini, P.J. Baker et al., Developing the Muon Facilities at ISIS, in *Proceedings of the 14th International Conference on Muon Spin Rotation, Relaxation and Resonance (μSR2017)*, Sapporo, Japan, 25–30 June 2017. https://doi.org/10.7566/JPSCP.21.011055
8. Y. Miyake, K. Shimomura, N. Kawamura et al., Current status of the J-PARC muon facility, MUSE, Paper presented at the 13th International Conference on Muon Spin Rotation, Relaxation and Resonance, Grindelwald, Switzerland, 1–6 June 2014. https://doi.org/10.1088/1742-6596/551/1/012061
9. A. Sato, Y. Kuno, H. Sakamoto et al., MuSIC, the world's highest intensity DC muon beam using a pion capture system, in *Conference proceedings of the 2nd International Particle Accelerator Conference (IPAC)*, San Sebastian, Spain, 4-9 September 2011. http://accelconf.web.cern.ch/AccelConf/IPAC2011/papers/MOPZ001.PDF
10. J.Y. Tang, S.N. Fu, J. Wei, Characteristics and potential applications of the proton beams at the CSNS. J. Korean Phys. Soc. **52**, 710–713 (2008). https://doi.org/10.3938/jkps.52.710
11. H.T. Jing, C. Meng, J.Y. Tang et al., Production target and muon collection studies for an experimental muon source at CSNS. Nucl. Instrum. Meth. A **684**, 109–116 (2012). https://doi.org/10.1016/j.nima.2012.05.045
12. R. Xiao, Y.F. Liu, X.J. Ni et al., Spin polarization and production rate studies of surface muons in a novel solenoid capture system based on CSNS. Nucl. Sci. Tech. **28**, 109 (2017). https://doi.org/10.1007/s41365-017-0261-4
13. E. Won, A proposal muon facility in RAON/Korea, in *Proceedings of the International Symposium on Science Explored by Ultra Slow Muon (USM213)*, Matsue, Shimane, Japan, 9–12 August 2014. https://doi.org/10.7566/JPSCP.2.010110
14. J.Y. Tang, X.J. Ni, X.Y. Ma et al., EMuS muon facility and its application in the study of magnetism. Quantum Beam Sci. **2**, 23 (2018). https://doi.org/10.3390/qubs2040023
15. K.M. Kojima, T. Murakami, T. Takahashi et al., New μSR spectrometer at J-PARC MUSE based on Kalliope detectors. Paper presented at the 13th International Conference on Muon Spin Rotation, Relaxation and Resonance, Grindelwald, Switzerland, 1–6 June 2014. https://doi.org/10.1088/1742-6596/551/1/012063
16. K. Sedlak, R. Scheuermann, T. Shiroka et al., MuSRSim and MusrSimAna—Simulation Tools for μSR Instruments. Phys. Procedia **30**, 61–64 (2012). https://doi.org/10.1016/j.phpro.2012.04.040
17. S. Agostinelli et al., Geant4—a simulation toolkit. Nucl. Instrum. Meth. A **53**, 250–303 (2003). https://doi.org/10.1016/S0168-9002(03)01368-8
18. R. Brun, F. Rademakers, ROOT—an object-oriented data analysis framework. Nucl. Instrum. Meth. A **389**, 81–86 (1997). https://doi.org/10.1016/S0168-9002(97)00048-X
19. S.R. Giblin, S.P. Cottrell, P.J.C. King et al., Optimising a muon spectrometer for measurements at the ISIS pulsed muon source. Nucl. Instrum. Meth. A **751**, 70–78 (2014). https://doi.org/10.1016/j.nima.2014.03.010
20. T.J. Roberts, D.M. Kaplan, G4beamline simulation program for matter-dominated beam lines. Paper presented at 2007 IEEE Particle Accelerator Conference (PAC), Albuquerque, NM, USA, 25–29 June 2007. https://doi.org/10.1109/PAC.2007.4440461
21. Nagamine, K, *Introductory Muon Science*. (Cambridge University Press, Cambridge, 2003), pp. 11–12. https://doi.org/10.1017/CBO9780511470776.002https://doi.org/10.1017/CBO9780511470776.002
22. Z. Pan, X. Ni, B. Ye, Conceptual design of MuSR spectrometer for EMuS using Monte Carlo simulation, in *Conference proceedings of 3rd China-Japan Joint Workshop on Positron Science (JWPS2017)*, Hefei, China, 8–10 June 2017. https://doi.org/10.7567/JJAPCP.7.011303
23. R.J. da Silva Afonso, P.J. Baker, J.S. Lord, et al, Monte Carlo simulations of the MuSR spectrometer at ISIS: current instrument and future designs. (STFC ePubs website, 2001) https://nmi3.eu/index.php?get_file=monte_carlo_simulations_of_the_musr_spectrometer_at_isis.pdf. Accessed 10 April 2019
24. Stephen Cottrell, Chinese Detector Tests, STFC ISIS Neutron and Muon Source, 2018. https://doi.org/10.5286/ISIS.E.RB1830641